
RESEARCH ARTICLE

Analysis of Element Composition of DNA-Protein Crystals *In Vitro*

A. V. Moiseenko^a, N. G. Loiko^{b,c}, O. V. Chertkov^a, A. V. Feofanov^{a,d},
Yu. F. Krupyanskiĭ^c, and O. S. Sokolova^{a,*}

^a Department of Biology, Moscow State University, Moscow, 119234 Russia

^b Research Center of Biotechnology, Russian Academy of Sciences, Moscow, 119071 Russia

^c Semenov Institute of Chemical Physics, Russian Academy of Sciences, Moscow, 117977 Russia

^d Shemyakin and Ovchinnikov Institute of Bioorganic Chemistry, Russian Academy of Sciences, Moscow, 117997 Russia

*e-mail: sokolova@mail.bio.msu.ru

Received July 7, 2019; revised August 11, 2019; accepted September 17, 2019

Abstract—The universal response of *Escherichia coli* to stress is enhancing the synthesis of specific histone-like Dps proteins that bind bacterial DNA. As a result, two-dimensional and three-dimensional crystalline arrays can be observed in the cytoplasm of starving bacteria. Conditions for obtaining *in vitro* co-crystals of DNA-Dps were selected, and their elemental composition was studied using analytical electron microscopy. It was found that Dps in the co-crystal retains its ferritin-like activity; that is, it can stimulate the oxidation of Fe²⁺ ions to Fe³⁺ and facilitate the accumulation of iron in the form of Fe₂O₃ in the inner cavity of the oligomer.

Keywords: *E. coli*, nucleoid, Dps, analytical electron microscopy, biocrystallization, fluorescence microscopy.

DOI: 10.3103/S0096392519040102

INTRODUCTION

The Dps protein is produced in *Escherichia coli* cells and belongs to the class of oxidoreductases, which oxidize metal ions [1]. A recent screening has revealed genomic regions in bacterial DNA that are primarily responsible for Dps binding [2]. Sites with affinity for Dps overlap with sites responsible for interacting with other DNA-binding proteins, including RNA polymerases. Thus, it was assumed that Dps can modulate the transcription of the bacterial chromosome [3], preventing the synthesis of RNA from some sites through competition with RNA polymerase or, conversely, thought competing with inhibitors, activating transcription. Dps interacts with DNA not inhibiting transcription, but restricting DNA access to other proteins, such as restriction endonucleases.

Dps protein synthesis is enhanced during the transition of *E. coli* to the stationary growth phase [1]. In this phase, highly ordered and stable DNA-Dps co-crystals are formed. Within the crystals, bacterial DNA is condensed and protected from various damage. Dps protects the genetic apparatus of a bacterial cell from ultraviolet and gamma radiation, temperature stress, and acid and base shock [4].

This mechanism, apparently, provides for the resumption of bacterial cell growth with the improve-

ment of external conditions [5]. Tightly packed, condensed DNA-Dps particles of various morphology were found in ultrathin sections of dormant *E. coli* cells, archaea, endospores of *B. thuringiensis* and *Br. laterosporus*, exospores of streptomycetes, arthro-bacter cells, and pseudomonads [6]. Persistent cells in populations of pathogenic bacteria, and which are multidrug-resistant, probably also have a crystalline nucleoid, which, may insure their resistance to antibiotics.

It is assumed that the efficient formation of DNA-Dps co-crystals is supported by different contents of divalent cations in successive phases of bacterial cell growth. In particular, in the log growth the DNA-Dps interaction can be inhibited by a low concentration of Mg²⁺ ions, while, in turn, it can be activated by a high concentration of these ions in the stationary phase [7]. It has also been previously shown that the addition of Fe²⁺ ions stabilizes the main functional oligomeric form of the Dps protein [8]. However, the effect of divalent cations on the structure of DNA-Dps co-crystals *in vitro* has not been studied yet. The true conformation of DNA in nanocrystalline DNA-Dps complexes is also unknown. We used fluorescently labeled DNA fragments, which allowed us to select the conditions for obtaining thin co-crystals of DNA-Dps

in vitro [9]. In this work, we studied the elemental composition of DNA-Dps co-crystals obtained in the presence of iron and zinc ions using analytical electron microscopy.

MATERIALS AND METHODS

Assembling labeled DNA template. A 165 bp fluorescently labeled DNA template containing the s603 sequence was obtained by polymerase chain reaction (PCR), as described previously [9]. DNA purification was carried out using a PCR product purification kit (Sigma), following the manufacturer's instructions. DNA concentration was determined by optical density at the 260 nm wavelength. The concentration was 0.25 µg/µL. As a result, labeled DNA with the following sequence was obtained:

AGCGACACCGGCACTGGGCCCCGGTTCGC-
GCTCCCGCCTTCCGTGTGTTGTCGTCTCTC-
GGGCGTCTAAGTACGCTTAGCGCACGGTA-
GAGCGCAATCCAAGGCTAACCACCGTG-
CATCGATGTTGAAAGAGGCCCTCCGTCCTTA
TTACTTCAAGTCCCTGGGGT

Expression and purification of the Dps protein was performed according to the protocol described previously [8]. For this purpose, the *E. coli* strain BL21-Gold was transformed with the pET-DPS plasmid. The LB culture medium (Lysogeny broth; supplemented with 150 mg/L ampicillin and 10 mM lactose) was inoculated with a single bacterial colony and incubated for 16–18 hr in a shaker-incubator at 37°C. Cells were pelleted by centrifugation (5000g, 15 min), resuspended in a 0.1 M Tris-HCl buffer (pH 7.5), and destroyed with an ultrasonic disintegrator. The lysate was centrifuged at 13000g for 10 min. The supernatant was purified by ion exchange chromatography on DEAE-Sephadex-A25 resin. Further purification was performed by gel filtration on Sephadex-G200 and by salting out the protein, followed by dialysis against a buffer containing 0.2 M NaCl, 20 mM Tris-HCl (pH 7.5).

Obtaining co-crystals of DNA-Dps in vitro. Co-crystals were obtained by mixing purified Dps protein (3.4 mg/mL) with a linear fluorescently-labeled DNA fragment (0.25 ng/µL). For fluorescence studies, 3 µL of a Dps solution was added to 3 µL of DNA in a silicone well, followed by 3 µL of an aqueous EDTA solution (0.14 mM), and 1 µL of an aqueous solution (10 mM) of one of the salts: FeCl₃, K₄[Fe(CN)₆], or ZnSO₄. The Dps to DNA ratio was 14 : 1.

For TEM (transmission electron microscopy) studies, co-crystals were formed directly on a TEM grid. Thus, a drop (1.5 µL) of purified Dps was added to a drop (1.5 µL) of DNA deposited on a carbon-coated copper grid (SPI, United States). Then, 1.5 µL of EDTA (0.14 mM) was added to the mixture to form crystals. To study the effect of iron and zinc cations on

crystals, 0.5 µL of 10 mM of one of the solutions—FeCl₃, K₄[Fe(CN)₆], or ZnSO₄—was added to the mixture.

Confocal microscopy. The effectiveness of the interaction of Dps with DNA was evaluated by the fluorescence method in the wells of a chamber attached to a coverslip. Images were obtained using an LSM710-Confocor3 inverted confocal laser scanning microscope (Zeiss, Germany) with a C-Apochromat ×40/1.20 water immersion lens. Fluorescence was excited by a laser with a wavelength of 514.5 nm, and was detected in the range of 524–639 nm. Lateral and axial resolutions were 0.2 and 0.6 µm, respectively.

Electron microscopy. TEM studies were performed on a JEM-2100 transmission electron microscope (JEOL, Japan) equipped with a lanthanum hexaborite (LaB6) cathode, operating at an accelerating voltage of 200 kV. The objective aperture was 40 µm. Images were obtained on a Gatan Ultrascan 1000FTXP detector with a 2K × 2K matrix size at a real magnification of 48200× (for samples with FeCl₃ and K₄[Fe(CN)₆]) and 6425× (for samples with ZnSO₄).

Electron energy loss spectroscopy (EELS). To obtain the spectra, a Gatan GIF Quantum ER spectrometer (Gatan, United States) was used. The input aperture of the spectrometer is 5 mm. The expected spectral resolution, measured by the half-width of the peak of zero loss, is no worse than 1.2 eV.

The spectrometer was used in the diffraction-coupled mode: the projection system of the microscope in the mode of energy-filtered transmission electron microscopy (EFTEM), and the signal collection angle was limited by an objective aperture of 10 mrad. The area on the sample for the collection of spectra was limited by a selective diffraction aperture (SAD) or by the input aperture of the spectrometer, in the case of small magnification.

A Fe L_{2,3} peak at a shift of 708 eV was selected to detect Fe, and a Zn L_{2,3} peak at a shift of 1020 eV was selected for zinc detection. The L_{2,3} peaks of transition metals in the EELS spectra have a good signal-to-noise ratio, which enables to detect very small atomic concentrations of these elements. However, the small scattering cross section for L_{2,3} peaks and their characteristic structure (“white lines”) complicates the accurate calculation of the scattering cross sections and, as a result, the quantitative analysis of the content of the selected elements [10].

The following parameters were used to obtain spectra in the region of the L_{2,3} iron peak: microscope magnification 48200×, dispersion 0.05 eV/channel at 2048 channels, 698–800 eV spectrum range, exposure time of one spectrum 30 sec, summation over 10 spectra.

For a set of spectra in the region of the zinc L_{2,3} peak, we used a magnification of 6425×, a dispersion

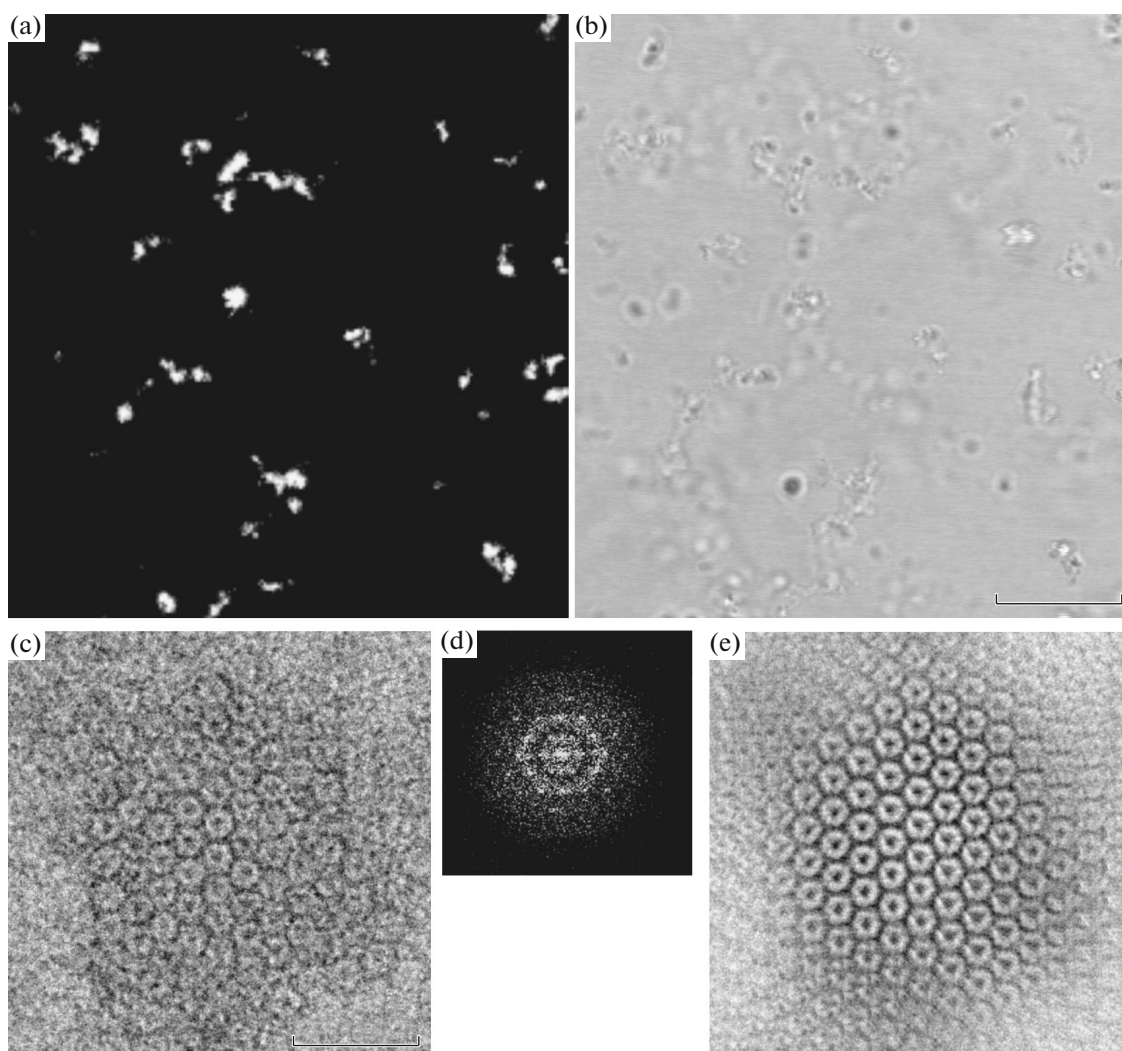


Fig. 1. Co-crystals of DNA-Dps in the presence of EDTA and FeCl_3 . (a) Co-crystals of DNA-Dps observed with a confocal microscope, fluorescence image; (b) Transmitted-light image of the same area; scale bar – 50 μm . (c) TEM image of negatively-stained DNA-Dps co-crystal; scale bar—50 nm. (d) Fourier transform from the selected area; (e) filtered projection image of a DNA-Dps co-crystal.

of 0.25 eV/channel at 2048 channels, a spectrum range of 870–1382 eV, 5 sec exposure time, a summation over 10 spectra, 60 μm objective aperture, limiting the signal collection angle up to no less than 20 mrad.

On each of the samples, a preliminary local control was performed using the EFTEM method to assess the need for introducing corrections for multiple scattering. The thickness of all samples was within 0.2 free paths of an electron for a given accelerating voltage. Therefore, corrections for multiple scattering were not applied.

The background component was removed in all the EELS spectra. It was extrapolated using a power function with an input window of 698–705 eV for iron spectra and 870–1000 eV for zinc spectra. The spectra

were processed in the “Digital Micrograph” software package (Gatan, United States).

RESULTS AND DISCUSSION

The process of biocrystallization of a nucleoid during the starvation of prokaryotic cells has previously been studied by cryoelectron microscopy [11] and X-ray diffraction analysis [12]. However, there is still disagreement over the true conformation of DNA within nanocrystalline DNA-Dps complexes in cells. This question is important since it is related to the organization of genetic material, which affects the translation and expression of genes, and, therefore, is critical for the functioning of organisms.

The use of a fluorescently labeled DNA fragment allowed us to observe DNA-Dps co-crystals directly in

Table 1. Linear dimensions of crystals observed under a confocal microscope depend on the ionic composition of the solution

Co-crystal formation conditions	Control (EDTA)	Fe ²⁺	Fe ³⁺	Zn ²⁺
Size*, μm	1.8 \pm 1.0	2.8 \pm 1.4	3.6 \pm 2.7	2.6 \pm 1.9
Confidence interval	0.25	0.35	0.3	0.8

* Mean \pm standard deviation.

solution (Fig. 1). Since the formation of co-crystals is affected by the concentration of divalent cations [7], we added a chelating agent EDTA at a concentration of 0.14 mM to the mixture and immediately (no more than 2–5 min) observed the formation of small fluorescent formations (Table 1). The addition of divalent Zn²⁺ cations in the form of ZnCl₂ or Fe²⁺ in the form of K₄[Fe(CN)₆] led to a slight increase in the linear sizes of these fluorescence formations, while adding trivalent Fe³⁺ in the form of FeCl₃ increased the dimensions of such formations by two times.

TEM with negative staining of the samples confirmed that the fluorescent formations observed in the solution possess a crystalline structure (Figs. 1c–1e) with clear particle shapes, with sizes corresponding to the size of the Dps dodecamer [1]. This suggests that co-crystals contain both DNA and Dps.

Survey EELS spectra of samples with FeCl₃ and K₄[Fe(CN)₆] demonstrated maxima in the region of the L_{2,3} peak of iron at 710 and 723 eV; however, the intensities of these maxima turned out to be extremely low. A lower intensity was observed on samples with ZnSO₄ at the L_{2,3} peak of zinc. This indicates that the concentration of iron and zinc in co-crystals is insufficient to construct the distribution maps of atoms of these elements by the method of energy-filtered images. Mapping using the STEM–EELS method (STEM–scanning transmission electron microscopy) was also impossible, due to the strong drift and damage of the samples by a high-intensity electron beam in the STEM during data acquisition. Therefore, the TEM–EELS method that limits the data set area by a selective aperture was chosen to obtain information on the spatial distribution of iron and zinc atoms.

Figures 2d–2f show the EELS spectra of a sample with FeCl₃ obtained both from sites containing protein–DNA co-crystals and from those lacking them (Figs. 2a–2c). The spectra contain peaks at 709 and 722 eV, corresponding to L₃ and L₂ peaks of iron. Both spectra were obtained under the same conditions. It has been seen that a signal along the L_{2,3} line of iron in the empty regions of the sample is present, but has a significantly lower intensity than in regions with DNA–Dps co-crystals. In accordance with data

on the structure of the L₃ peak of iron [13], it can be concluded that iron atoms are in the 3+ oxidation state. A peak at 707 eV corresponding to iron in the 2+ oxidation state is absent in the obtained spectra. It should also be mentioned that the spectra obtained from all the samples contain intense maxima at 740 and 782 eV. They most likely correspond to the M₄ line of Cs and the M₅ line of Ba. These elements may be included as impurities in the uranyl acetate used for negative contrasting.

Figures 2g, 2h represent the EELS spectra of the sample with K₄[Fe(CN)₆]. To improve the signal-to-noise ratio, a larger selective aperture of 100 μm was chosen. In this sample, the intensity of the L_{2,3} peak of iron relative to the intensity of the M₄ peak of cesium (Cs) is significantly lower than in the sample with FeCl₃. It can be seen that the position of the L₃ peak also corresponds to the iron in the 3+ oxidation state. There is no signal from iron 2+ in the spectrum.

Dps catalytic centers oxidize iron ions in the free state. Oxidized iron penetrates into the internal cavity of the Dps protein, forming an inorganic core [2]. We suppose that something like this can happen with Dps, being a part of a co-crystal with DNA. In the crystalline state, Dps, apparently, can also stimulate the accumulation of iron in the form of Fe₂O₃ (or Fe₃O₄) in the inner cavity of the oligomer. Thus, the data obtained expand the idea of the role of Dps in the cell.

The spectra from samples with ZnSO₄ are shown in Figs. 2i, 2j. A peak at 1043 eV is observed, which corresponds to the position of the L_{2,3} peak of zinc. However, the intensity of this peak was low. This reaffirms the evidence that Dps does not permanently bind divalent cations (except iron, which it oxidizes), and that this process is dynamic in nature [7].

Thus, using a fluorescently labeled DNA fragment and confocal laser microscopy, the formation of DNA–Dps co-crystals in a solution containing iron ions is shown. When comparing our experimental data with the data for purified Dps protein [2], it was suggested that the Dps in the co-crystal retains its ferritin-like activity; that is, it can stimulate the oxidation of Fe²⁺ ions to Fe³⁺ and promote the accumulation of iron in the form of Fe₂O₃ (or Fe₃O₄) in the inner cavity of the oligomer, as shown

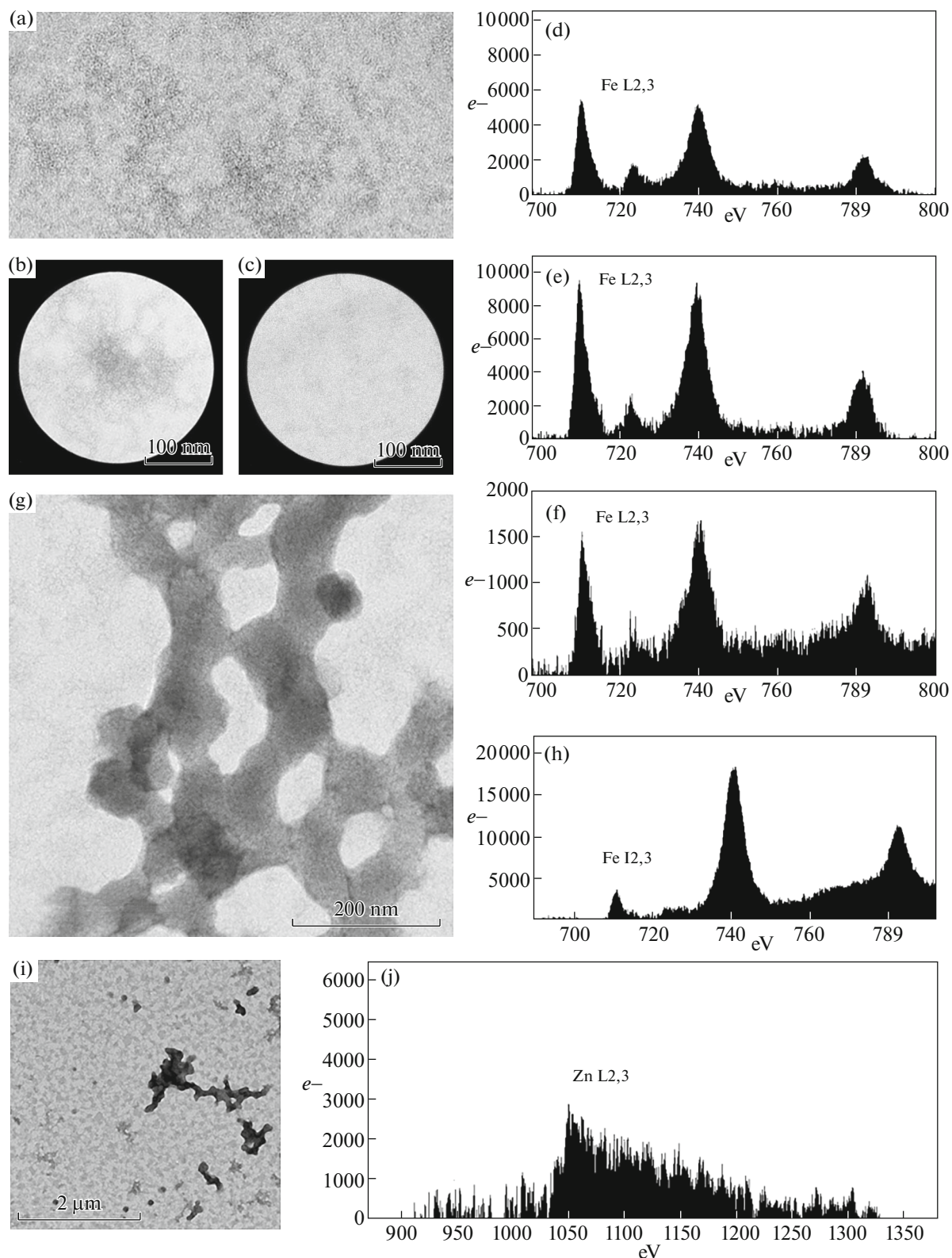


Fig. 2. Element analysis of DNA-Dps co-crystals. (a) TEM image of a region of a sample with DNA-Dps co-crystals containing FeCl₃; scale bar – 100 nm. (b) A region limited by a selective aperture containing DNA-Dps co-crystals. (c) A region limited by a selective aperture without co-crystals. EELS spectra in the range of the L_{2,3} peak of iron corresponding to regions (a–c). (g) TEM image of a region of the sample with DNA-Dps co-crystals with K₄[Fe(CN)₆] limited to a selective aperture of 100 μm. (h) The EELS spectrum in the region of the L_{2,3} peak of iron from section g. (i) The region of the sample with ZnSO₄ containing DNA-Dps co-crystals. (j) Corresponding EELS spectrum containing a L-2,3 zinc peak.

previously. These data can further be used to study the three-dimensional organization of the genetic material in bacterial cells.

ACKNOWLEDGMENTS

Analytical electron and fluorescence microscopy were performed with the financial support from the Russian Science Foundation (project no. 19-74-30003). The expression and purification of the Dps protein was carried out as part of the state task of the Russian Ministry of Education and Science (topic 0082-2014-0001, no. AAAA-A17-117040610310-6, and topic 0104-2019-0005). The electron microscopy was carried out using a JEOL2100 analytical electron microscope (JEOL, Japan) as part of a unique research facility “Three-Dimensional Electron Microscopy and Spectroscopy” of the Faculty of Biology of Moscow State University.

CONFLICT OF INTEREST

The authors declare that they do not have a conflict of interest.

COMPLIANCE WITH ETHICAL STANDARDS

The study was performed without the use of animals or people as subjects.

REFERENCES

1. Almiron, M., Link, A.J., Furlong, D., and Kolter, R., A novel DNA-binding protein with regulatory and protective roles in starved *Escherichia coli*, *Genes Dev.*, 1992, vol. 6, pp. 2646–2654.
2. Antipov, S.S., Tutukina, M.N., Preobrazhenskaya, E.V., Kondrashov, F.A., Patrushev, M.V., Toschakov, S.V., Dominova, I., Shvyreva, U.S., Vrublevskaya, V.V., Moronkov, O.S., Sukharicheva, N.A., Panyukov, V.V., and Ozoline, O.N., The nucleoid protein Dps binds genomic DNA of *Escherichia coli* in a nonrandom manner, *Plos One*, 2017, vol. 12, no. 8.
3. Shen, B.A. and Landick, R., Transcription of bacterial chromatin, *J. Mol. Biol.*, 2019, vol. 2836, no. 19.
4. Martinez, A. and Kolter, R., Protection of DNA during oxidative stress by the nonspecific DNA-binding protein Dps, *J. Bacteriol.*, 1997, vol. 179, no. 16, pp. 5188–5194.
5. Minsky, A., Shimoni, E., and Frenkiel-Krispin, D., Stress, order and survival, *Nat. Rev. Mol. Cell Biol.*, 2002, vol. 3, pp. 50–60.
6. Loiko, N.G., Suzina, N.E., Soina, V.S., Smirnova, T.A., Zubasheva, M.V., Azizbekyan, R.R., Sinitsyn, D.O., Tereshkina, K.B., Nikolaev, Y.A., Krupyanskiy, Y.F., and El'-Registan, G.I., Biocrystalline structures in nucleoids of stationary and dormant cells of procarior, *Micromicrobiology*, 2017, vol. 86, no. 6, pp. 714–727.
7. Frenkiel-Krispin, D., Levin-Zaidman, S., Shimoni, E., Wolf, S.G., Wachtel, E.J., Arad, T., Finkel, S.E., Kolter, R., and Minsky, A., Regulated phase transitions of bacterial chromatin: A non-enzymatic pathway for generic DNA protection, *EMBO J.*, 2001, vol. 20, no. 5, pp. 1184–1191.
8. Antipov, S., Turishchev, S., Purtov, Y., Shvyreva, U., Sinelnikov, A., Semov, Y., Preobrazhenskaya, E., Berezhnoy, A., Shusharina, N., Novolokina, N., Vakh-tel, V., Artyukhov, V., and Ozoline, O., The oligomeric form of the *Escherichia coli* Dps protein depends on the availability of iron ions, *Molecules*, 2017, vol. 22, no. 11.
9. Moiseenko, A., Loiko, N., Tereshkina, K., Danilova, Y., Kovalenko, V., Chertkov, O., Feofanov, A.V., Krupyanskiy, Y.F., and Sokolova, O.S., Projection structures reveal the position of the DNA within DNA-Dps co-crystals, *Biochem. Biophys. Res. Commun.*, 2019, vol. 517, no. 3, pp. 463–469.
10. Egerton, R.F., *Electron Energy-Loss Spectroscopy in the Electron Microscope*, New York: Springer, 2011, 3rd ed.
11. Dadinova, L.A., Chesnokov, Y.M., Kamyshinsky, R.A., Orlov, I.A., Petoukhov, M.V., Mozhaev, A.A., Soshinskaya, E.Y., Lazarev, V.N., Manuvera, V.A., Orekhov, A.S., Vasiliev, A.L., and Shtykova, E.V., Protective Dps-DNA co-crystallization in stressed cells: An in vitro structural study by small-angle X-ray scattering and cryo-electron tomography, *FEBS Lett.*, 2019, vol. 593, no. 12, pp. 1360–1371.
12. Loiko, N.G., Danilova, Ya.A., Moiseenko, A.V., Demkina, E.V., Kovalenko, V.V., Tereshkina, K.B., El-Registan, G.I., Sokolova, O.S., and Krupyanskiy, Yu.F., Condensation of nucleoid in *Escherichia coli* cell as a result of prolonged starvation, *ArXiv Quant. Biol.*, 2019, vol. 1901.
13. Garvie, L.A.J., Craven, A.J., and Brydson, R., Use of electron-energy loss near-edge fine structure in the study of minerals, *Am. Mineral.*, 1994, vol. 79, no. 5–6, pp. 411–425.